

NUMERICAL PREDICTION OF THE COMPOUND LAYER GROWTH DURING THE GAS NITRIDING OF Fe-M BINARY ALLOYS

NUMERIČNO NAPOVEDOVANJE RASTI SPOJINSKE PLASTI MED PLINSKIM NITRIRANJEM BINARNIH ZLITIN Fe-M

Ramdane Kouba, Mourad Keddam

Laboratoire de Technologie des Matériaux, Département SDM, Faculté de Génie Mécanique et Génie des Procédés, USTHB BP 32 El-Alia
16111 Alger, Algeria
r_kouba1@yahoo.fr

Prejem rokopisa – received: 2013-10-03; sprejem za objavo – accepted for publication: 2014-01-20

A numerical model was developed to simulate the gas nitriding of Fe-M binary alloys. The suggested model takes into account the nitrogen diffusion in the compound layer and in the diffusion zone as well as the displacement of the (γ'/α) interface. The precipitation of fine MN nitrides in the diffusion zone was also considered during the modelling. A numerical resolution of the problem was done with the front-tracking method via the finite-difference technique. The model was capable of predicting the growth of the γ' -compound layer and also the nitrogen-depth profile. In order to validate the model, the compound-layer thicknesses obtained with the simulation were compared with those obtained experimentally for the nitrided Fe-Cr binary alloys. Good concordance between the numerical results and the experimental data was noticed.

Keywords: gas nitriding, modelling, compound layer, front-tracking method

Razvit je bil numerični model za simulacijo plinskega nitriranja binarnih zlitin Fe-M. Predlagani model upošteva difuzijo dušika v spojinski plasti in tudi v difuzijski plasti, kot tudi premik stika (γ'/α). Model upošteva tudi izločanje drobnih MN-nitridov v difuzijski coni. Numerična rešitev problema je bila izvršena z uporabo metode sledenja fronte z uporabo tehnike končnih diferenc. Model je sposoben predvidevanja rasti γ' spojinskega sloja in tudi profila dušika v globino. Za oceno modela je bila pri simulaciji dobljena debelina spojinske plasti primerjana z eksperimentalno dobljeno debelino pri nitriranih binarnih zlitinah Fe-Cr. Ugotovljeno je dobro ujemanje med numeričnimi rezultati in eksperimentalnimi podatki.

Ključne besede: nitriranje v plinu, modeliranje, spojinski sloj, metoda sledenja fronte

1 INTRODUCTION

Gas nitriding is a thermochemical process in which nitrogen atoms diffuse into the material surface after the dissociation of ammonia gas. The nitriding temperature varies between 500 °C and 600 °C with the time duration ranging from a few hours to a few days.

After this treatment, the nitride layers are formed and we can distinguish a compound layer and a diffusion zone. The compound layer, also called the white layer, generally contains two sublayers: the γ' phase, mainly composed of iron nitride (Fe_4N) and the ε phase as $\text{Fe}_2\text{N}_{1-x}$. The thickness of the compound layer can reach a value of 50 μm . Beneath the compound layer, the diffusion zone can extend up to a depth of 1200 μm . For binary alloys, the diffusion zone is a ferrite which contains atomic nitrogen dissolved interstitially, with dispersed fine metallic nitrides of the MN type where M is a nitride-forming element. This diffusion zone is responsible for increasing the resistance to fatigue observed after nitriding.

The main objective of modelling nitriding is to quantitatively describe different phenomena occurring during the gas-nitriding treatment. Several models¹⁻⁷ were reported in the literature, describing the nitriding

process for iron alloys and steels. These models allowed the prediction of the nitriding kinetics and microstructure of the nitrided zone.

Most of these models focus on the diffusion zone, in which nitrogen diffusion takes place simultaneously with the precipitation of the nitrides of the MN type (where M is an alloying element). In the case of steels, the presence of carbides and carbonitrides was also considered in the modelling⁵ on the basis of the appropriate thermodynamic data.

However, these models did not take into account the presence of the compound layer, despite the fact that the formation of this layer has an important influence on the properties of a nitrided material. Indeed, the white layer can lead to a significant improvement in tribological and anti-corrosion properties⁸. In the case of the nitriding of steels, it has been shown that the microstructure of the compound layer has an influence on the hardening depth in the diffusion zone⁹. With respect to these considerations, it is interesting to include this layer in the modelling.

The prediction of the nitriding process including several phases (ε , γ' and α) was already achieved for the case of nitrided pure iron. This modelling was performed

analytically and reported on in¹⁰⁻¹³, while the numerically performed modelling was described in¹⁴⁻¹⁸. However, a corresponding model of nitriding a multi-component system, such as Fe-M binary alloys and steels, is not yet available.

The main objective of the present work is to present such a model, relating to the gas nitriding of a Fe-M binary alloy. However, the numerical approach developed in the present work only deals with a single compound layer consisting of γ' nitride.

2 MATHEMATICAL FORMULATION OF THE MODEL

During the gas nitriding of pure iron and binary alloys or even steels, the formation of the compound layer depends on the operating parameters, particularly, the nitriding potential r_N (see references^{15,16} for further details). In fact, three configurations are possible:

- the absence of the compound layer (and therefore the treatment is completed in the ferritic phase)
- the compound zone with a single-phase γ'
- the compound zone with a dual-phase (ϵ/γ').

In the present work, the aim was to simulate the nitriding process with the presence of only γ' in the compound zone. Therefore, the chosen value of r_N must correspond to this configuration according to the Lehrer diagram¹⁶.

During the nitriding treatment, if the thermodynamic conditions are satisfied, γ' precipitates appear in the vicinity of the external surface if the solubility limit of nitrogen in ferrite is reached. Thereafter, the γ' phase tends to grow at the expense of the ferrite. This phase transformation ($\alpha \rightarrow \gamma'$) involves a displacement of the (γ'/α) interface.

A diffusion problem, with one or more moving boundaries, is commonly called the Stefan problem. Its solving is usually performed with the use of one of the front-tracking methods.

In¹⁹⁻²² several models based on this approach are presented in order to simulate phase transformations in metals and alloys. The model presented in²⁰ was implemented in the DICTRA software and used to simulate the nitriding process in a Fe-N system^{13,14}.

In the present work, a new front-tracking method is presented considering both the long-range diffusion in the diffusion zone and the interstitial diffusion of nitrogen within the iron nitrides. The nitrogen diffusion takes place simultaneously with the advancement of the (γ'/α) interface.

It should be noted that the diffusion of heavy elements (Fe, M) was neglected as the nitrogen diffusion controls the growth of the compound layer. This hypothesis has already been adopted by several authors¹⁻⁷.

The main objective of the present model is to simulate the growth of the γ' layer at the expense of ferrite. However, in the diffusion zone, the nitrogen diffusion

occurs simultaneously with the precipitation of MN nitrides which also affect the growth kinetics of the γ' layer. For this reason, this precipitation phenomenon was also included in the modelling.

After the γ' phase is precipitated, the problem can be represented schematically as shown in **Figure 1**, where the two phases, γ' and α , are henceforth adjacent. At any time t , the position of the interface (γ'/α) is represented by the distance λ from the origin ($z = 0$) which corresponds to the (γ'/gas) interface.

The nitrogen diffusion in each phase is governed by the Fick's second law. The system of Equations 1 and 2 can be established in the one-dimensional space as:

$$\frac{\partial N_{\gamma'}}{\partial t} = \frac{\partial}{\partial z} \left(D_{\gamma'}(N_{\gamma'}) \frac{\partial N_{\gamma'}}{\partial z} \right) \text{ in the } \gamma' \text{ phase} \quad (1)$$

$$\frac{\partial N_{\alpha}}{\partial t} = \frac{\partial}{\partial z} \left(D_{\alpha}(N_{\alpha}) \frac{\partial N_{\alpha}}{\partial z} \right) \text{ in the } \alpha \text{ phase} \quad (2)$$

where $N_{\gamma'}$ and N_{α} represent, respectively, the nitrogen concentrations in the γ' and α phases. These concentrations are expressed as the numbers of moles per unit volume and they are dependent on the depth (z) and time (t). The nitrogen amount can also be expressed as a nitrogen mole fraction ($X_{\gamma'}$, X_{α}) using the relations: $N_{\gamma'} = X_{\gamma'}/V_{\gamma'}$ and $N_{\alpha} = X_{\alpha}/V_{\alpha}$, where $V_{\gamma'}$ and V_{α} are the molar volumes of the two phases that are considered independent of the compositions. The concentration may also be converted into mass fractions.

$D_{\gamma'}(N_{\gamma'})$ and $D_{\alpha}(N_{\alpha})$ are defined as the nitrogen diffusion coefficients dependent on the N amount.

During the incremental time dt the interface position advances with the value of $d\lambda$. In order to conserve the number of nitrogen moles and considering the nitrogen flux arriving at the interface and the nitrogen flux leaving the interface, the following balance equation can be established (Equation 3):

$$(X_{\gamma'\alpha} - X_{\alpha\gamma'}) \frac{v}{V_{\gamma'}} = \left[-D_{\gamma'} \frac{\partial N_{\gamma'}}{\partial z} \right]_{z=\lambda} - \left[-D_{\alpha} \frac{\partial N_{\alpha}}{\partial z} \right]_{z=\lambda} \quad (3)$$

Where v is the interface velocity expressed as $v = d\lambda/dt$.

The terms $X_{\alpha\gamma'}$ and $X_{\gamma'\alpha}$ are the nitrogen molar fractions at the interface of the two phases, α and γ' , respectively (refer to **Figure 1**). It is assumed that the thermodynamic equilibrium is continuously established between the two phases, α and γ' at the considered interface. So, $X_{\alpha\gamma'}$ and $X_{\gamma'\alpha}$ can be read from the corresponding phase diagram.

The diffusion problem with the moving boundaries is then governed by the set of three partial differential equations (Equations 1, 2 and 3). The solving of the problem of interest requires the knowledge of the following boundary conditions:

In the external surface ($z = 0$), the nitrogen concentration in γ' is considered constant (N_s) corresponding to

the equilibrium between γ' and the gas mixture. Therefore, at $z = 0$, $N_{\gamma'}(0,t) = N_s$, at $z = \lambda$, $N_{\gamma'}(\lambda,t) = N_{\gamma'\alpha}$ and $N_{\alpha}(\lambda,t) = N_{\alpha\gamma'}$.

For greater depths (i.e., $z > 1200 \mu\text{m}$), this zone corresponds to the non-nitrided core where the nitrogen amount in the matrix is neglected. Therefore, at $z = +\infty$, $N_{\alpha}(\infty,t) = 0$.

3 NUMERICAL SOLVING OF THE PROBLEM

The finite-difference method is used to solve the problem of the nitrogen diffusion with a moving boundary. For this purpose, the zones occupied by both phases, γ' and α , are divided into the cells with thicknesses $\Delta z_{\gamma'}$ and Δz_{α} , respectively, as shown in **Figure 1**. Two adjacent cells are separated by a node. It is assumed that at time t , the number of nodes in the γ' phase is $n_{\gamma'}$ and in α it is n_{α} (the numbers of cells in both phases will then be $(n_{\gamma'} - 1)$ and $(n_{\alpha} - 1)$, respectively).

The thicknesses of all the cells are kept constant except for the last cell in γ' and the first cell in the α phase, which are considered as time-dependent during

the simulation process (**Figure 1**). Indeed, as the interface advances, there is an expansion of the left cell and shrinkage of the one on the right. By introducing these two variable cells, it becomes possible to follow the progress of the γ'/α interface during the numerical calculation as explained below.

When using the finite-difference method, the time is also discretized with an equal time step (Δt). The solution is assumed to be known at time t , then it is calculated at the next time step ($t + \Delta t$). At the instant t , the nitrogen concentration in each node is known for both γ' and α and so are the sizes of the two variable cells, $d_{\gamma'}(t)$ and $d_{\alpha}(t)$.

In order to determine these values at time $(t + \Delta t)$, the process can be divided in two steps: first, a diffusion step where the nitrogen diffusion occurs in γ' and α by considering the displacement of the (γ'/α) interface.

In the diffusion step, the resolution consists of separate solutions of diffusion Equations 1 and 2 in their corresponding areas. This allows a determination of the nitrogen concentration profile for the whole nitrided zone.

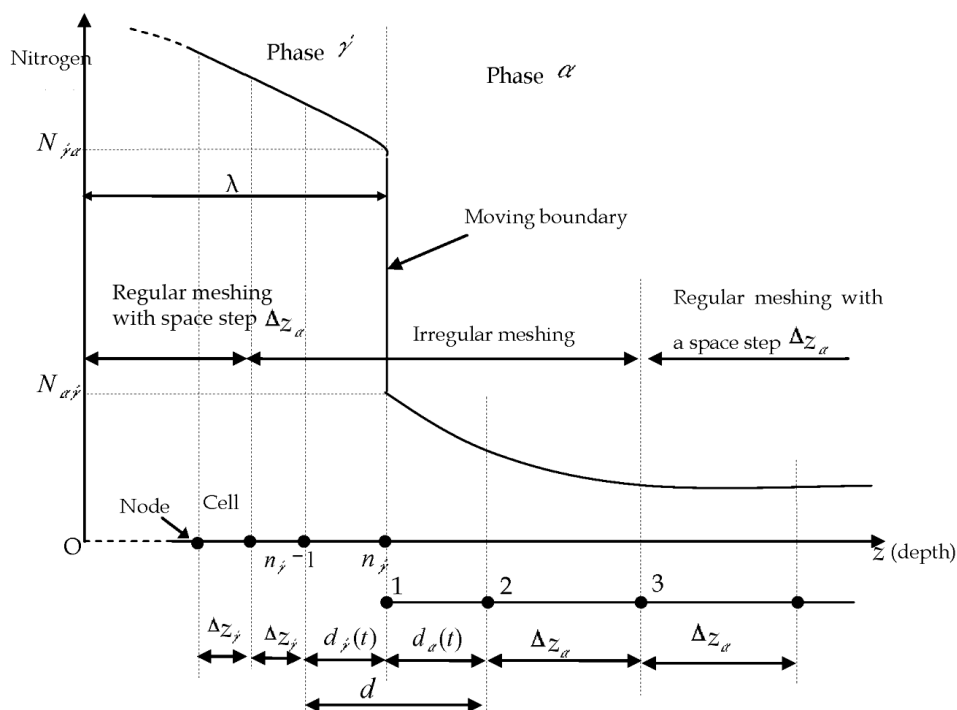


Figure 1: Schematic diagram illustrating the problem of nitriding with the presence of γ' as the compound layer. In order to carry out a numerical resolution, the zone occupied by the two phases, γ' and α , is divided into small cells. Two adjacent cells are separated by a node also called a grid point. It is supposed that the number of nodes is equal to $n_{\gamma'}$ and n_{α} in the γ' phase and α phase, respectively. In order to consider the displacement of the interface, the thicknesses of the last cell in γ' and the first cell in α are considered variable during the process. When the cell on the right-hand side dilates, the left one shrinks, while the sum ($d_{\gamma'} + d_{\alpha}$) remains constant being equal to d .

It should be noted that all the nodes of the grid are immobile, except for the last node in γ' and the first one in α , which are mobile. At the interface, the N concentration is kept constant in both phases with the values of $N_{\gamma'\alpha}$ and $N_{\alpha\gamma'}$. The corresponding N mole fractions (i.e., $X_{\gamma'\alpha}$ and $X_{\alpha\gamma'}$) can be read from the phase diagram.

Slika 1: Shematski prikaz problema pri nitriranju s prisotnostjo spojinske plasti γ' . Za numerično resolucijo je bila plast, v kateri sta dve fazi, γ' in α , razdeljena v majhne celice. Dve sosednji celici sta ločeni z vozlov oz. točko v mreži. Predvideva se, da je število vozlov enako $n_{\gamma'}$ in n_{α} v γ' -fazi in α -fazi. Da bi upoštevali premik stične ploskve, se kot spremenljivki v procesu vzameta debelina zadnje celice v γ' in prve celice v α . Medtem ko se celica na desni strani širi, se na levi oži. Medtem pa vsota ($d_{\gamma'} + d_{\alpha}$) ostaja konstantna in je enaka d .

Treba je omeniti, da so vsi vozli v mreži nemobilni, razen zadnjega vozla v γ' in prvega v α , ki sta mobilna. Na stiku je koncentracija N konstantna v obeh fazah z vrednostima $N_{\gamma'\alpha}$ in $N_{\alpha\gamma'}$. Ustrezni molski deleži N (to je $X_{\gamma'\alpha}$ in $X_{\alpha\gamma'}$) se prebere iz faznega diagrama.

In order to solve the diffusion equation in γ' using the finite-difference technique, Equation 1 is rewritten in the following form:

$$\frac{\partial N_{\gamma'}}{\partial t} = D_{\gamma'}(N_{\gamma'}) \frac{\partial^2 N_{\gamma'}}{\partial z^2} + \left(\frac{\partial D_{\gamma'}(N_{\gamma'})}{\partial z} \right) \left(\frac{\partial N_{\gamma'}}{\partial z} \right) \quad (4)$$

When the implicit scheme is used, a relation between the unknown nitrogen concentrations in three successive nodes ($i-1$, i and $i+1$) can be found. This is done simply by replacing the partial derivatives, which appear in Equation 4, with their corresponding finite differences^{23,24}. The following relation can be established:

$$A_i N_{\gamma'}(i-1, t+\Delta t) + B_i N_{\gamma'}(i, t+\Delta t) + C_i N_{\gamma'}(i+1, t+\Delta t) = N_{\gamma'}(i, t) \quad 2 \leq i \leq n_{\gamma'} - 2 \quad (5)$$

The values for A_i , B_i and C_i are obtained with the following expressions:

$$A_i = \frac{[D_{\gamma'}(i+1) - D_{\gamma'}(i+1) - 4D_{\gamma'}(i)] \Delta t}{4(\Delta z_{\gamma'})^2}$$

$$B_i = 1 + \frac{2D_{\gamma'}(i) \Delta t}{(\Delta z_{\gamma'})^2}$$

$$C_i = -\frac{[D_{\gamma'}(i+1) + D_{\gamma'}(i+1) + 4D_{\gamma'}(i)] \Delta t}{4(\Delta z_{\gamma'})^2}$$

Obviously, the diffusion coefficient $D_{\gamma'}$ changes along the depth, so the term $D_{\gamma'}(i)$ corresponds to its value at the node i . The variation of the diffusion coefficient in γ' with the nitrogen amount is described in **Appendix 1**.

Equation 5 is valid for a regular meshing with the same cell size, $\Delta z_{\gamma'}$. However, in the vicinity of the γ'/α interface, due to the presence of the variable cell, the mesh is irregular. Therefore, the relation between the N concentrations in the last three nodes in γ' is not given by Equation 5. An equivalent equation can be obtained by replacing partial derivatives with finite differences in Equation 4 as follows:

$$\frac{\partial^2 N_{\gamma'}}{\partial z^2} \Big|_{z=z_{\gamma'\alpha-1}} = \frac{2N_{\gamma'}(n_{\gamma'} - 2, t+\Delta t)}{\Delta z_{\gamma'} [d_{\gamma'} + \Delta z_{\gamma'}]} - \frac{2N_{\gamma'}(n_{\gamma'} - 1, t+\Delta t)}{\Delta z_{\gamma'} d_{\gamma'}} + \frac{2N_{\gamma'}(n_{\gamma'}, t+\Delta t)}{d_{\gamma'} [d_{\gamma'} + \Delta z_{\gamma'}]} \quad (6)$$

$$\frac{\partial N_{\gamma'}}{\partial z} \Big|_{z=z_{\gamma'\alpha-1}} = \frac{N_{\gamma'}(n_{\gamma'}, t+\Delta t) - N_{\gamma'}(n_{\gamma'} - 2, t)}{d_{\gamma'} + \Delta z_{\gamma'}} \quad (7)$$

$$\frac{\partial D_{\gamma'}}{\partial z} \Big|_{z=z_{\gamma'\alpha-1}} = \frac{D_{\gamma'}(n_{\gamma'}) - D_{\gamma'}(n_{\gamma'} - 2)}{d_{\gamma'} + \Delta z_{\gamma'}} \quad (8)$$

$$\frac{\partial N_{\gamma'}}{\partial t} \Big|_{z=z_{\gamma'\alpha-1}} = \frac{N_{\gamma'}(n_{\gamma'} - 1, t+\Delta t) - N_{\gamma'}(n_{\gamma'} - 1, t)}{\Delta t} \quad (9)$$

By substituting these relations (6 to 9) in Equation 4, Equation 10 can be obtained as follows:

$$A_{n_{\gamma'}-1} N_{\gamma'}(n_{\gamma'} - 2, t+\Delta t) + B_{n_{\gamma'}-1} N_{\gamma'}(n_{\gamma'} - 1, t+\Delta t) + C_{n_{\gamma'}-1} N_{\gamma'}(n_{\gamma'}, t) = N_{\gamma'}(n_{\gamma'} - 1, t) \quad (10)$$

$$A_{n_{\gamma'}-1} = \left[\frac{D_{\gamma'}(n_{\gamma'}) - D_{\gamma'}(n_{\gamma'} - 2)}{(d_{\gamma'} + \Delta z_{\gamma'})^2} - \frac{2D_{\gamma'}(n_{\gamma'})}{\Delta z_{\gamma'} (d_{\gamma'} + \Delta z_{\gamma'})} \right] \Delta t$$

$$B_{n_{\gamma'}-1} = 1 + \frac{2D_{\gamma'}(n_{\gamma'}) \Delta t}{\Delta z_{\gamma'} d_{\gamma'}}$$

$$C_{n_{\gamma'}-1} = \left[\frac{D_{\gamma'}(n_{\gamma'} - 2) - D_{\gamma'}(n_{\gamma'})}{(d_{\gamma'} + \Delta z_{\gamma'})^2} - \frac{2D_{\gamma'}(n_{\gamma'})}{\Delta z_{\gamma'} (d_{\gamma'} + \Delta z_{\gamma'})} \right] \Delta t$$

Equations 5 and 10 represent a set of $(n_{\gamma'} - 2)$ equations with $(n_{\gamma'} - 2)$ unknowns. In order to determine the nitrogen concentrations in the nodes at time $(t + \Delta t)$ this set of equations must be solved using the tridiagonal matrix algorithm (TDMA)²³.

The same analysis can be applied for the numerical solution of the diffusion equation in the ferritic phase (Equation 2). However, it was shown in several references¹⁵⁻¹⁸ that the dependence of the diffusion coefficient on the composition of ferrite is weak. So, in the present paper, a constant value for diffusivity is adopted and noted as D_{α} .

The following relation can be established for the first three nodes in the ferritic phase (irregular mesh, similar to Relation 10):

$$A_2^{\alpha} N_{\alpha}(2, t+\Delta t) + B_2^{\alpha} N_{\alpha}(3, t+\Delta t) = N_{\alpha}(2, t) \quad (11)$$

$$A_2^{\alpha} = \frac{-2D_{\alpha} \Delta t}{d_{\alpha} (d_{\alpha} + \Delta z_{\alpha})}, \quad B_2^{\alpha} = 1 + \frac{2D_{\alpha} \Delta t}{\Delta z_{\alpha} d_{\alpha}}$$

$$C_2^{\alpha} = \frac{-2D_{\alpha} \Delta t}{\Delta z_{\alpha} (d_{\alpha} + \Delta z_{\alpha})}$$

For the other nodes (for $i = 2$ to $n_{\alpha} - 1$) a relationship similar to (5) can be given:

$$-r_{\alpha} N_{\alpha}(i-1, t+\Delta t) + (1+2r_{\alpha}) N_{\alpha}(i, t+\Delta t) - r_{\alpha} N_{\alpha}(i+1, t+\Delta t) = N_{\alpha}(i, t) \quad (12)$$

$$\text{where } r_{\alpha} = \frac{D_{\alpha} \Delta t}{(\Delta z_{\alpha})^2}$$

As for the γ' phase, the resolution of the set of Equations 11 and 12 indicates the nitrogen concentration in each node of the ferritic phase at time $(t + \Delta t)$.

4 CONSIDERING THE DISPLACEMENT OF THE (γ'/α) INTERFACE

After the diffusion step, the nitrogen concentration in both phases is modified. The change in the nitrogen profile leads to a displacement of the corresponding interface so that the nitrogen-amount balance is conserved.

Equation 3 which gives the interface velocity must then be included into the resolution.

The main feature associated with the present model and compared to most of the other front-tracking methods (given, for example, in¹⁹⁻²¹) is the inclusion of the diffusion near the interface. The diffusion process near the interface region was already considered in the modelling from reference²². In the present work, the simplest method is used to take this phenomenon into account. For this purpose, it is supposed that the interface is governed not only by Relation 3 but also by Diffusion Equations 1 and 2. In fact, near the interface, the three partial differential equations, 1, 2 and 3, are solved simultaneously.

The technique used in the resolution consists of replacing the partial derivatives with their finite differences. But at this time, the sizes of variable cells are time-dependent and are still unknown at $t + \Delta t$.

For example, to get the diffusion equation for γ' , in the finite-difference form near the interface, (according to an implicit scheme), we simply substitute Relations 6 to 9 into 4 given that the term $d_{\gamma'}$ is considered at the time $t + \Delta t$ and not at t . The following equation can be obtained:

$$\frac{N_{\gamma'}(n_{\gamma'}-1, t+\Delta t) - N_{\gamma'}(n_{\gamma'}-1, t)}{\Delta t} = 2D_{\gamma'}(n_{\gamma'}-1) \cdot \left\{ \frac{N_{\gamma'}(n_{\gamma'}-2, t+\Delta t)}{\Delta z_{\gamma'} [d_{\gamma'}(t+\Delta t) + \Delta z_{\gamma'}]} - \frac{N_{\gamma'}(n_{\gamma'}-1, t+\Delta t)}{\Delta z_{\gamma'} d_{\gamma'}(t+\Delta t)} \right. \\ \left. - \frac{N_{\gamma'\alpha}}{d_{\gamma'}(t+\Delta t) [d_{\gamma'}(t+\Delta t) + \Delta z_{\gamma'}]} \right\} + \frac{[N_{\gamma'\alpha} - N_{\gamma'}(n_{\gamma'}-2, t+\Delta t)] \cdot [D_{\gamma'}(n_{\gamma'}) - D_{\gamma'}(n_{\gamma'}-2)]}{[d_{\gamma'}(t+\Delta t) + \Delta z_{\gamma'}]^2} \quad (13)$$

It should be noted that this relationship is similar to 10, but in this case $d_{\gamma'}$ is still unknown at the $(t + \Delta t)$ instant.

Similarly, the diffusion Equation 2 can be written near the interface as finite differences. Then the following relation can be established:

$$\frac{N_{\alpha}(2, t+\Delta t) - N_{\alpha}(2, t)}{\Delta t} = 2D_{\alpha} \left\{ \frac{N_{\alpha\gamma'}}{d_{\alpha}(t+\Delta t) [d_{\alpha}(t+\Delta t) + \Delta z_{\alpha}]} - \frac{N_{\alpha}(2, t+\Delta t)}{\Delta z_{\alpha} d_{\alpha}(t+\Delta t)} \right. \\ \left. + \frac{N_{\alpha}(3, t+\Delta t)}{\Delta z_{\alpha} [d_{\alpha}(t+\Delta t) + \Delta z_{\alpha}]} \right\} \quad (14)$$

The thickness of the shrinking cell $d_{\alpha}(t + \Delta t)$ is not an independent variable, but it is related to $d_{\gamma'}(t + \Delta t)$ with the following relation (**Figure 1**):

$$d_{\alpha}(t + \Delta t) = d - d_{\gamma'}(t + \Delta t) \quad (15)$$

By substituting Equation 15 into 14, the discrete form of Equation 2 can be given near the interface as follows:

$$\frac{N_{\alpha}(2, t+\Delta t) - N_{\alpha}(2, t)}{\Delta t} = 2D_{\alpha} \left\{ \frac{N_{\alpha\gamma'}}{[d - d_{\gamma'}(t + \Delta t)] \cdot [d - d_{\gamma'}(t + \Delta t) + \Delta z_{\alpha}]} - \frac{N_{\alpha}(2, t+\Delta t)}{\Delta z_{\alpha} [d - d_{\gamma'}(t + \Delta t)]} + \frac{N_{\alpha}(3, t+\Delta t)}{\Delta z_{\alpha} [d - d_{\gamma'}(t + \Delta t) + \Delta z_{\alpha}]} \right\} \quad (16)$$

Finite differences are also determined in the case of Equation 3 and the following relations can then be written:

$$\frac{\partial N_{\gamma'}}{\partial z} \Big|_{z=\lambda} = \frac{N_{\gamma'\alpha} - N_{\gamma'}(n_{\gamma'}-1, t+\Delta t)}{d_{\gamma'}(t+\Delta t)} \quad (17)$$

$$\frac{\partial N_{\alpha}}{\partial z} \Big|_{z=\lambda} = \frac{N_{\alpha}(2, t+\Delta t) - N_{\alpha\gamma'}}{d_{\alpha}(t+\Delta t)} \quad (18)$$

In order to write the derivative $d\lambda/dt$ as a finite difference, it is worth noting that the change in the position of the interface is related only to the change in the expanding cell size. So, the following relation can be written:

$$\frac{d\lambda}{dt} = \frac{d(d_{\gamma'})}{dt} = \frac{d_{\gamma'}(t+\Delta t) - d_{\gamma'}(t)}{\Delta t} \quad (19)$$

Substituting these three last relations (17, 18 and 19) into Equation 3, the following relation can be obtained:

$$d_{\gamma'}(t + \Delta t) - d_{\gamma'}(t) = \frac{\Delta t V_{\gamma'}}{(X_{\gamma'\alpha} - X_{\alpha\gamma'})} \cdot \left\{ D_{\gamma'}(n_{\gamma'}) \frac{N_{\gamma'}(n_{\gamma'}-1, t+\Delta t) - N_{\gamma'\alpha}}{d_{\gamma'}(t+\Delta t)} - D_{\alpha} \frac{N_{\alpha\gamma'} - N_{\alpha}(2, t+\Delta t)}{[d - d_{\gamma'}(t+\Delta t)]} \right\} \quad (20)$$

The above analysis has finally led to the set of three nonlinear equations (13, 16 and 20) with the following unknowns: $d_{\gamma'}(t + \Delta t)$, $N_{\gamma'}(n_{\gamma'} - 1, t + \Delta t)$ and $N_{\gamma'}(2, t + \Delta t)$. So, after the diffusion step, the consideration of the interface displacement is performed by solving this set of equations in order to determine the corresponding unknowns. The resolution requires the use of an iterative algorithm with the Newton-Raphson method.

Once the resolution is achieved (i.e., $d_{\gamma'}(t + \Delta t)$ is calculated), the interface position at the time $(t + \Delta t)$ can be determined from Equation 21:

$$\lambda(t + \Delta t) = \lambda(t) + d_{\gamma'}(t + \Delta t) - d_{\gamma'}(t) \quad (21)$$

The term $\Delta\lambda = d_{\gamma'}(t + \Delta t) - d_{\gamma'}(t)$ represents the advancement of the interface during a time step.

The thickness of the shrinking cell is also calculated by using Relation 15.

The two steps of the resolution (i.e., the nitrogen diffusion and the interface displacement) are afterwards repeated for the next time step.

It should be mentioned that the nitrogen concentration in the first neighbouring nodes of the interface (i.e., $N_{\gamma'}(n_{\gamma'} - 1, t + \Delta t)$ and $N_{\gamma'}(2, t + \Delta t)$) is computed in both diffusion step and interface-displacement step. For the next time step, only the values resulting from the interface-displacement analysis are retained.

During the simulation process, there is an expansion of the left cell and shrinkage of the one on the right. However, this process cannot continue indefinitely and the remeshing may become necessary if $d_{\gamma'}$ is too large or d_{α} becomes too small. So, the two following criteria have been adopted: The expanding cell splits into two cells if its size becomes 1.5 times greater than the original size. This division is performed by inserting a new node inside the cell. The nitrogen concentration in the new node is obtained with a linear interpolation from the concentration in the neighbouring nodes. Similarly, if the shrinking cell reaches half of its original size, a grid point is removed from α in order to increase d_{α} to its initial value. It can be seen that when the simulation process is performed, there is a creation of nodes and cells in phase γ' and a disappearance of others in α .

5 APPLICATION OF THE MODEL FOR THE NITRIDED Fe-M BINARY ALLOYS

In fact, the configuration presented in **Figure 1** does not appear at the first instant at the beginning of the nitriding process, but there is a period of nitrogen enrichment in the ferrite which precedes the formation of the compound layer.

This incubation time is more important when the M alloying element is present in the ferritic matrix because of the consumption of a large amount of nitrogen in the MN nitride precipitation. In addition, if the nitriding potential r_N is not too high, as assumed in the present work, the incubation time is even longer²⁵. For these reasons, the early stage of the process, which takes place completely in the ferritic phase, must be considered.

Before the γ' formation, the diffusion of nitrogen is carried out exclusively in the ferrite zone according to Equation 2. In this case, at $z = 0$, there is a ferrite/gas contact. The transfer of nitrogen from the gas mixture to the metal is expressed with the following relationship:

At $z = 0$,

$$-D_{\alpha} \left. \frac{\partial N_{\alpha}}{\partial z} \right|_{z=0} = K_{\alpha} [N_{eq\alpha} - N_{\alpha}(0, t)] \quad (22)$$

Equation 22 is obtained by considering a thermodynamic equilibrium between the solid (the α phase) and the gas mixture. The term $N_{eq\alpha}$ indicates the nitrogen concentration in ferrite at the thermodynamic equilibrium between α and the gas mixture. $N_{\alpha}(0, t)$ represents the actual concentration at the surface and K_{α} is the

kinetic constant. Equation 22 is regarded as an external boundary condition when solving the diffusion problem in the preliminary stage.

The nitriding process during the preliminary stage can be regarded as the nitrogen diffusion in one phase (ferrite) coupled to the precipitation of fine MN nitrides. The details of the calculation procedure are given in¹. After the diffusion step which causes a modification of the nitrogen profile, a test of the MN precipitation is realized at each depth using the solubility-product method. So, the amount of the nitrogen precipitated as MN and the quantity which remains dissolved in the ferrite can be calculated. It is also possible to determine the proportion of M consumed by the precipitation and the residual part dissolved in the matrix¹.

The nitrogen transfer from the gas mixture to the sample, according to Equation 22, means that the N concentration in the ferrite at $z = 0$ increases with time. The formation of γ' takes place when the surface concentration reaches the solubility limit of the nitrogen in ferrite. Therefore, the condition of the precipitation of γ' on the top of α , at $z = 0$, is satisfied if: $N_{\alpha}(0, t) \geq N_{\alpha\gamma'}$. This test is performed for each time step during the calculation process in the preliminary stage.

It should be noted that the kinetic considerations related to the γ' nucleation have been neglected which makes the formation of the compound layer take place as soon as the nitrogen solubility limit is reached.

Subsequently, a small γ' layer with a thickness not exceeding $0.1 \mu\text{m}$ is inserted at the top of the first cell of α having an initial thickness of $1 \mu\text{m}$.

The introduction of a small thickness of the γ' layer is the beginning of the diffusion problem with a moving boundary. Thereafter, the front-tracking solving process is conducted as explained in detail in Sections 3 and 4.

However, when solving a diffusion problem with moving boundaries for binary alloys, there is not just the nitrogen diffusion in the phase (ferrite) on the right, but

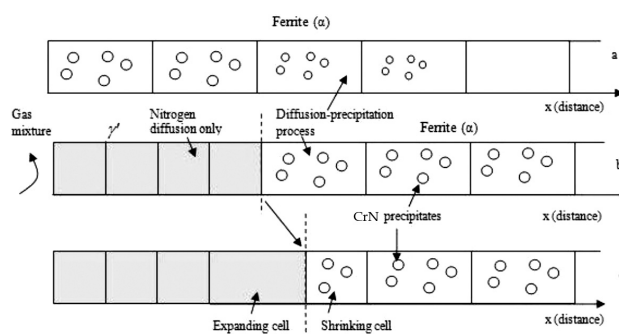


Figure 2: Schematic diagram illustrating a full simulation of nitriding Fe-Cr alloys. The diagram shows the formation of CrN precipitates and evolution of the variable cell size: a) during the early stage, b) after the formation of the compound layer (at time t_1), c) for a time $t_2 > t_1$

Slika 2: Shematski prikaz polne simulacije nitriranja zlitin Fe-Cr. Diagram prikazuje nastanek izločkov CrN in razvoj spremenljivke velikosti celic: a) v začetni fazi, b) po nastanku spojinske plasti (v času t_1), c) za čas $t_2 > t_1$

also the precipitation of MN nitrides which continues to occur after the γ' formation. The precipitation of MN nitrides is considered during the simulation in the same way as in the preliminary stage.

A schematic illustration of a full simulation of the gas nitriding of Fe-M binary alloys is shown in **Figure 2**. A general scheme giving different steps of the calculation is presented in **Figure 3**. A computer code written in the MATLAB language was used to achieve the numerical resolution and the necessary data for the implementation of the simulation are presented and discussed in **Appendix 2**.

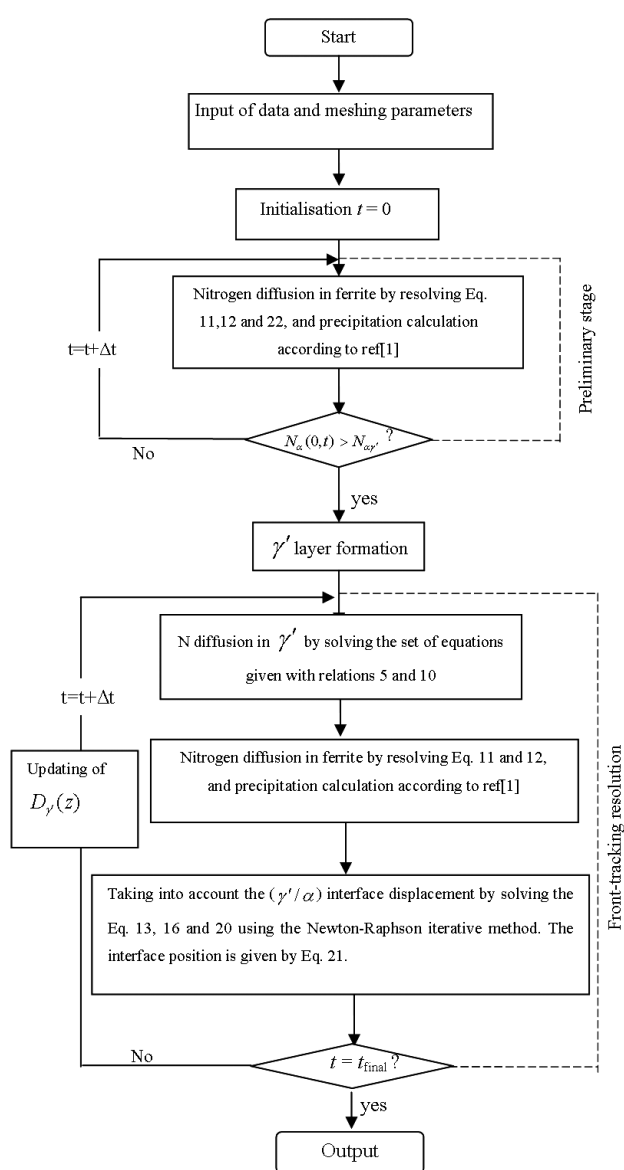


Figure 3: Flow chart showing a global scheme of the simulation of the nitriding process

Slika 3: Diagram prikazuje celotno shemo simulacije poteka postopka nitiranja

6 SIMULATION RESULT

Before presenting the results of the model for nitriding Fe-Cr binary alloys, the model was first applied to a Fe-N binary system. The case of nitriding pure iron is quite interesting since the analytical solution of the problem is already available¹⁰⁻¹². Therefore, a comparison between the results of the analytical model¹¹ and those obtained with the present work for Cr % = 0 is possible. For this purpose, a constant diffusion coefficient was adopted for γ' instead of the composition-dependent diffusivity. The same data, used in¹¹, was adopted for the numerical resolution and the incubation time was also ignored.

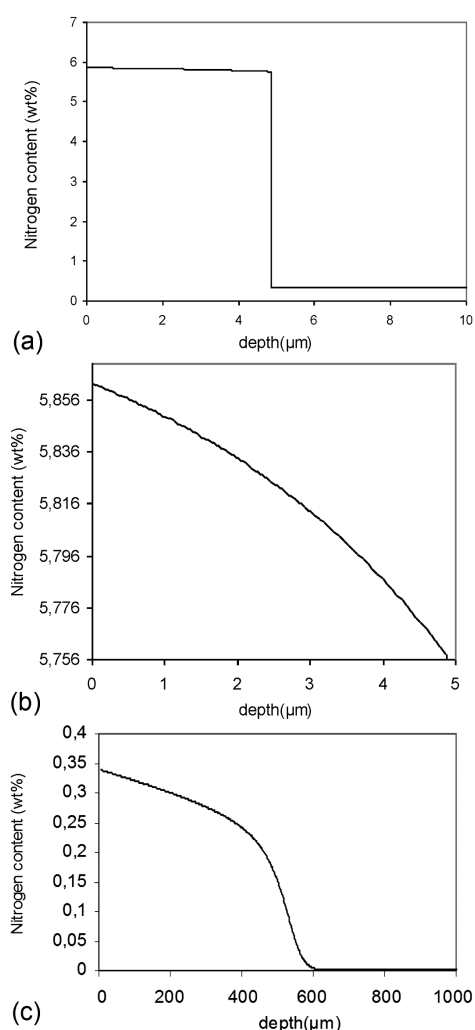


Figure 4: Results given by the model for the nitriding of Fe – 1 % Cr binary alloy for the given nitriding conditions: $T = 550$ °C, $r_N = 0.7$ bar^{-1/2}, time = 16 h: a) nitrogen-concentration profile for the compound layer and the beginning of the diffusion zone, b) profile of nitrogen inside the compound layer, c) total nitrogen profile for the diffusion zone

Slika 4: Rezultati, ki jih da model za nitiranje binarne zlitine Fe – 1 % Cr v danih razmerah nitiranja: $T = 550$ °C, $r_N = 0,7$ bar^{-1/2}, trajanje = 16 h: a) profil koncentracije dušika v spojinski plasti in začetek difuzijske cone, b) profil koncentracije dušika v spojinski plasti, c) skupni profil dušika v difuzijski coni

It is noticed that the numerical solution converges towards the analytical one provided that the spatial and temporal discretization steps are as small as possible. Indeed, the following parameters ($\Delta z_{\gamma'} = 0.1 \mu\text{m}$, $\Delta z_{\alpha} = 0.1 \mu\text{m}$ and $\Delta t = 0.1 \text{s}$) provide a good accuracy. These parameters were adopted for all the numerical calculations done in the present study. A good agreement between the numerical and analytical results represents, in fact, the first step in the validation of the model.

Figure 4a shows the simulated nitrogen-concentration profiles through the γ' layer and the beginning of the diffusion zone obtained after nitriding the Fe – 1 % Cr binary alloys (for the following conditions: $T = 550 \text{ }^\circ\text{C}$, $K_N = 0.7 \text{ bar}^{-1/2}$ and $t = 16 \text{ h}$).

For the compound layer, despite the narrow composition range, **Figure 4b** shows that the profiles are not linear, in contrast to the assumption made in¹⁵.

Figure 4c shows the total nitrogen profile within the diffusion zone. The major part of nitrogen is in the form of the CrN precipitate. The results are the same as those obtained in¹.

In this last reference¹, the experimental nitrogen profile fits well with the simulation results despite the fact that some aspects of the problem were not taken into account (for example, the nitrogen excess and the nucleation and growth kinetic of the formation of MN precipitates). These considerations can be seen as part of the validation of the present model with respect to the diffusion zone as long as the same solubility product K_{CrN} is used.

Figure 5 shows, for the same alloy and for two different temperatures (520 °C and 550 °C) the evolution of simulated compound-layer thickness versus time. In this figure, it is possible to deduce the corresponding values of incubation times, and to confirm the parabolic regime of the growth law of the γ' layer.

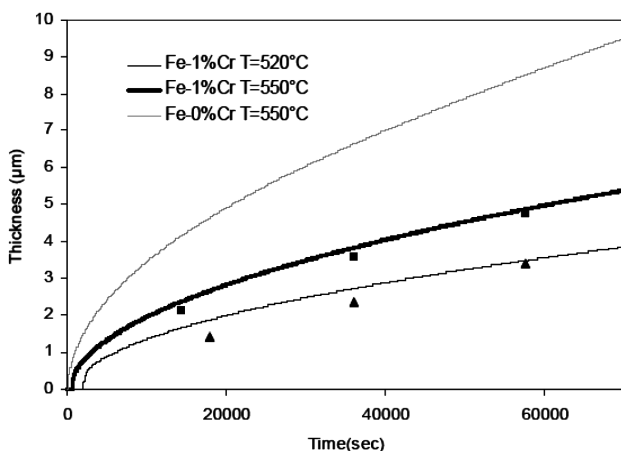


Figure 5: Comparison between the γ' layer thicknesses obtained with the model (curve) and those measured experimentally (marks) for $r_N = 0.7 \text{ bar}^{-1/2}$

Slika 5: Primerjava med debelino plasti γ' , dobljene z modelom (kriuljja) in eksperimentalno izmerjene (točke) pri $r_N = 0,7 \text{ bar}^{-1/2}$

In the same figure, the growth of the γ' layer in the case of the Fe-N system ($w(\text{Cr}) = 0 \%$) is also presented.

It can be seen that the presence of alloying element Cr slows down the growth of the compound layer. This result can be attributed to the CrN precipitation. Indeed, on the one hand, the precipitation reaction near the outer surface during the preliminary phase delays the formation of iron nitrides by increasing the corresponding incubation time. On the other hand, the CrN precipitation accentuates the nitrogen concentration gradient in the ferrite near the interface (on the right-hand side) because of the consumption of a large amount of nitrogen initially dissolved in the ferrite. Thereafter, the nitrogen flux leaving the interface is increased which leads to a reduction in the interface velocity.

7 EXPERIMENTAL VALIDATION OF THE MODEL

In order to validate the model, nitriding experiments were carried out on the Fe – 1 % Cr binary alloy. The measurements of the compound-layer thicknesses were subsequently realized with the purpose of comparing them with the simulated results.

The samples of the Fe – 1 % Cr alloy were gas nitrided in the laboratory nitriding furnace at 520 °C and 550 °C during different treatment times for the same nitriding potential ($K_N = 0.7 \text{ bar}^{-1/2}$). The identification of the phases formed after nitriding was performed using X-ray diffraction. The measurements of the thicknesses were performed using a scanning electron microscope at different locations of the cross-sections of the nitrided samples. The mean value of the compound-layer thickness was then taken from different measurements.

Figure 6 shows a micrograph of the nitrided zone, where one can distinguish the compound layer and the beginning of the diffusion zone. **Figure 7** shows the X-ray diffraction pattern of the gas-nitrided sample at T

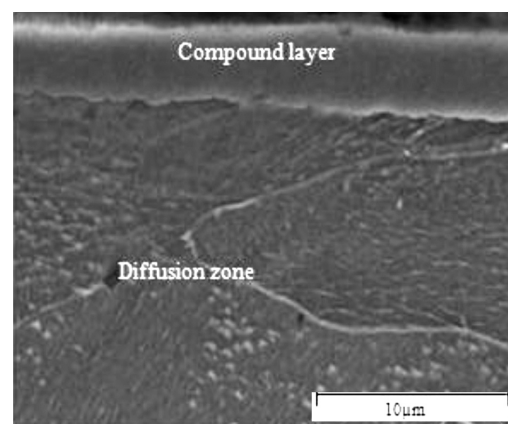


Figure 6: SEM micrograph of the cross-section of nitrided Fe – 1 % Cr alloy for the nitriding conditions: ($T = 550 \text{ }^\circ\text{C}$, $t = 10 \text{ h}$, $K_N = 0.7 \text{ bar}^{-1/2}$)

Slika 6: SEM-posnetek prereza nitrirane zlitine Fe – 1 % Cr pri rdezh nitriranja: ($T = 550 \text{ }^\circ\text{C}$, $t = 10 \text{ h}$, $K_N = 0,7 \text{ bar}^{-1/2}$)

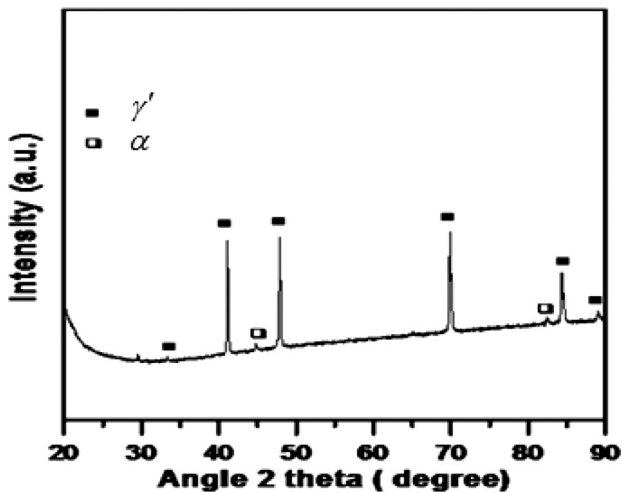


Figure 7: X-ray diffraction pattern of the surface of gas-nitrided Fe – 1 % Cr alloy at $T = 550\text{ }^{\circ}\text{C}$ during 10 h of treatment

Slika 7: Rentgenska difrakcija površine plinsko nitrirane zlitine Fe – 1 % Cr 10 h pri $T = 550\text{ }^{\circ}\text{C}$

= $550\text{ }^{\circ}\text{C}$ during 10 h of treatment. It can be seen that the detected phase includes γ' nitride and ferrite with no CrN which is probably due to its small fraction. It can also be seen that the nitriding conditions did not allow the formation of ϵ nitride.

The comparison between the experimental values of the γ' layer thicknesses and those calculated by the model is shown in Figure 5. It can be seen that there is good agreement between the experimental thicknesses and the simulated ones. This comparison leads to the conclusion that the model predicts, in a good way, the growth kinetics of the compound zone.

8 FURTHER POSSIBILITIES OF THE MODEL

The model provides good results concerning the growth of the compound layer, at least for the considered range of nitriding conditions and for low concentrations of the Cr alloying element. The model can be extended to perform a bilayer configuration (ϵ/γ') of the compound zone. The model can also be extended to simulate the nitriding of alloyed steel.

This requires a method for handling, the presence of several alloying elements with the possibility of different types of MN precipitates. The modeling of nitriding steels necessitates, especially, the consideration of the carbon element which brings significant changes to the microstructure before and during nitriding.

For example, it is reported in several studies^{5,26} that the alloyed carbides transform into nitrides or carbonitrides during the process and that the nitrogen interstitial diffusion is accelerated by that of carbon.

One of the solutions that can be adopted to simulate the nitriding of steels is to combine the present model with a thermodynamic model using the CALPHAD approach as shown in⁵ for the diffusion zone.

If the present model is interfaced with appropriate thermodynamic and kinetic data (resulting from thermodynamic calculations) it becomes a more complete model for the nitriding of steels. Such a model is able to predict nitrogen profiles in the diffusion zone and also in the compound layer.

Furthermore, the present model can be extended to study other processes involving moving boundaries, such as phase transformations and solidification. The model can even be extended to consider a case of a multicomponent system where several elements are able to diffuse as reported in^{20–22}. However, it requires the use of a comprehensive thermodynamic description necessary to determine different diffusivities and chemical potentials required for handling a diffusion process. However, in the present work, the model was restricted to the simulation of a nitriding process for binary alloys.

9 CONCLUSION

A numerical model for a simulation of the gas nitriding of Fe-M binary alloys is presented. The model takes into account both the diffusion precipitation in the diffusion zone and the nitrogen within the iron nitride γ' , also considering the (γ'/α) interface displacement. The diffusion problem with a moving boundary formulated in this way is solved through the front-tracking approach. Because of the presence of the M alloying element, the model also considers the precipitation of the MN nitrides in the diffusion zone. The numerical solving was achieved using the finite-difference method via an implicit scheme.

The numerical resolution allows a determination of the nitrogen profile along the depth as well as the interface position which makes it possible to follow the growth kinetics of the compound layer. There is a good concordance between the numerical calculations and the experimental results in the case of nitriding the Fe – 1 % Cr alloy.

Despite the fact that the model is limited to the case of a monolayer compound zone, it can be used as a tool for controlling the nitriding process and optimizing the desired properties.

Moreover, the applicability of the model can be extended to simulate the nitriding of steels using an appropriate thermodynamic and kinetic database in the simulation.

APPENDIX 1: VARIATION IN THE DIFFUSION COEFFICIENT IN γ' WITH THE COMPOSITION

The implementation of the model requires a determination of the dependence of the intrinsic diffusion coefficient on the nitrogen amount in the γ' phase. On the basis of thermodynamic and kinetic considerations, the following expression can be established:

$$D_{\gamma'}(N_{\gamma'}) = D_{\gamma'}^* \frac{d \ln a_N}{d \ln N_{\gamma'}} \quad (\text{A1})$$

where a_N is the nitrogen activity in γ' and $D_{\gamma'}^*$ is the nitrogen-tracer diffusion coefficient which is considered independent of the composition. The term $\Phi = \frac{d \ln a_N}{d \ln N_{\gamma'}}$ is often called the thermodynamic factor.

During the gas nitriding process with the presence of a gas mixture (NH_3/H_2), it is assumed there is a thermodynamic equilibrium between the solid (γ') and the atmosphere. It was shown that the activity of nitrogen is proportional to the nitriding potential of $r_N = P_{\text{NH}_3}/P_{\text{H}_2}$ ^{15,16}. The thermodynamic factor can then be rewritten as follows:

$$\Phi = \frac{d \ln r_N}{d \ln N_{\gamma'}} \quad (\text{A2})$$

Using the absorption-isotherm theory, Somers et al.¹⁵ gave the relation between the nitrogen amount in γ' and the nitriding potential, expressed with the following equation:

$$y_{N,\gamma'} = \frac{1}{4} \left\{ 1 + \left[\exp\left(-\frac{7558}{T} + 2.978\right) \right] \left[\frac{r_N}{r_{N,\gamma'}^0} - \frac{r_{N,\gamma'}^0}{r_N} \right] \right\} \quad (\text{A3})$$

where $y_{N,\gamma'}$ is the nitrogen amount expressed as a site fraction. The meanings and values of the constants appearing in A3 are given in the same reference¹⁵. In order to obtain the nitrogen concentration (the number of moles per volume), the following relationship can be used:

$$N_{\gamma'} = \frac{y_{N,\gamma'}}{V_{\gamma'}(1+y_{N,\gamma'})} \quad (\text{A4})$$

For each composition, Relations A3 and A4 can be combined and derived in order to calculate the thermodynamic factor Φ (according to A2) and then the corres-

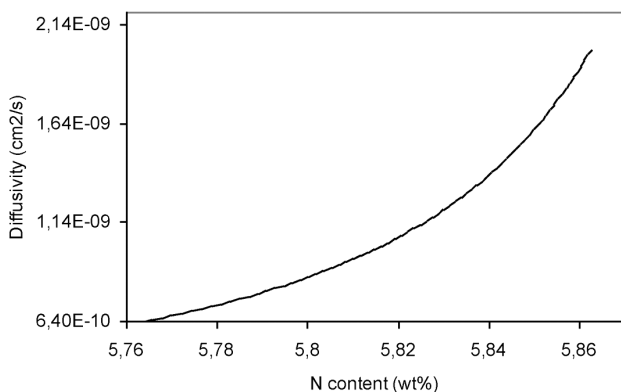


Figure 8: Evolution of the diffusion coefficient $D_{\gamma'}(N)$ versus the nitrogen concentration in γ' ($T = 550$ °C, $r_N = 0.7$ bar^{-1/2})

Slika 8: Razvoj koeficienta difuzije $D_{\gamma'}(N)$ v odvisnosti od koncentracije dušika v γ' ($T = 550$ °C, $r_N = 0,7$ bar^{-1/2})

ponding diffusivity (according to A1). In this way, the composition dependence of diffusivity was taken into account in the model and implemented as explained above.

Figure 8 shows the evolution of the diffusion coefficient $D_{\gamma'}$ versus the mass fraction of N, at $T = 550$ °C and $r_N = 0.7$ bar^{-1/2}. A strong dependence on the concentration can be observed.

APPENDIX 2: DATA USED IN THE SIMULATION

The data required for the simulation are gathered in **Table 1**.^{1,13,15,16,18,27} It is worth noting that when considering the nitrogen concentrations in both the external surface (N_s) and at the interface ($N_{\gamma'\alpha}$, $N_{\alpha\gamma'}$), the Fe-N binary phase diagram was used instead of an isothermal section of the Fe-N-Cr phase diagram.

Table 1: Different constants used for implementing the model with their source references

Tabela 1: Različne konstante, uporabljene v modelu in reference njihovih izvora

Constant	Value at 520 °C	Value at 550 °C	References
K_{α} /(cm/s)	5.3332 E-6	7.6047 E-6	27
$w(N_{eq\alpha})/\%$	0.1807	0.2742	15,16
$w(N_s)/\%$	5.8630	5.8621	15,16
$x(X_{\gamma'\alpha})/\%$	0.1973	0.1964	15,16
$x(X_{\alpha\gamma'})/\%$	0.0026	0.0032	15,16
$w(K_{CrN})/\%^{-2}$	0.0019	0.0033	1
D_{α} /(cm ² /s)	4.9183 E-8	7.5636 E-8	15,16
$D_{\gamma'}$ /(cm ² /s)	8.3870 E-12	1.3303 E-11	18
V_{α} /(cm ³ /mol)	7.14	7.14	13
$V_{\gamma'}$ /(cm ³ /mol)	8.22	8.22	13

mass fraction, $w/\%$

amount (= mol) fraction, $x/\%$

This was possible because during the preliminary phase the CrN precipitation near the external surface consumes practically all the dissolved Cr so that γ' nitride precipitates, thereafter, from the ferrite containing almost no alloying element. The CrN nitride is thermodynamically stable and assumed to be stoichiometric. This simplification was already adopted in¹.

In addition, in the Fe-N system the boundaries between phases were considered as a function of the nitriding potential instead of the total nitrogen amount. This phase diagram is called the Lehrer diagram and the corresponding thermodynamic description can be found in^{15,16}.

10 REFERENCES

- 1 Y. Sun, T. Bell, Materials Science and Engineering A, 224 (1997), 33–47
- 2 M. Gouné, T. Belmonte, J. M. Fiorani, S. Chomer, H. Michel, Thin Solid Films, 377–378 (2000), 543–549

- ³ H. P. Van Landeghem, M. Gouné, A. Redjaimia, *Journal of Crystal Growth*, 341 (2012), 53–60
- ⁴ R. Schacherl, P. C. J. Graat, E. J. Mittemeijer, *Metall. Mater. Trans.*, 35A (2004), 3387
- ⁵ S. Jegou, PhD thesis, ENSAM, Aix En Provence, France, 2009
- ⁶ J. D. Kamminga, G. C. A. M. Janssen, *Surface and Coatings Technology*, 200 (2006), 5896–5901
- ⁷ R. Kouba, M. Keddham, M. E. Djeghlal, *Journal of Alloys and Compounds*, 536 (2012), 124–131
- ⁸ H. C. F. Rozendaal, P. F. Colijn, E. J. Mittemeijer, *Surface Engineering*, 1 (1985), 30–43
- ⁹ J. Ratajski, R. Olik, *Advanced Materials Research*, 83–86 (2010), 1025–1034
- ¹⁰ M. Keddham, M. E. Djeghlal, L. Barralier, *Materials Science and Engineering A*, 378 (2004), 475–478
- ¹¹ L. Torchane, P. Bilger, J. Dulcy, M. Gantois, *Metallurgical and Materials Transactions A*, 27A (1996), 1823–1834
- ¹² M. Keddham, M. E. Djeghlal, L. Barralier, E. Salhi, *Annales de Chimie-Science des Matériaux*, 28 (2003), 53–61
- ¹³ H. Du, J. Ågren, *Metallurgical and Materials Transactions A*, 27A (1996), 1073–1080
- ¹⁴ H. Du, J. Ågren, *Z. Metallkunde*, 86 (1995), 522–529
- ¹⁵ M. A. Somers, E. J. Mittemeijer, *Metallurgical and Materials Transactions A*, 26A (1995), 57–74
- ¹⁶ E. J. Mittemeijer, M. A. J. Somers, *Surface Engineering A*, 13 (1997), 483–497
- ¹⁷ P. B. Friehling, M. A. J. Somers, *HTM J*, 57 (2002), 415–420
- ¹⁸ T. Belmonte, M. Gouné, H. Michel, *Materials Science and Engineering A*, 302 (2001), 246–251
- ¹⁹ T. C. Illingworth, I. O. Golosnoy, *Journal of Computational Physics*, 209 (2005), 207–225
- ²⁰ S. Crusius, G. Inden, U. Knoop, L. Höglund, J. Ågren, *Zeitschrift für Metallkunde*, 83 (1992), 673–678
- ²¹ H. Larsson, R. C. Reed, *Acta Materialia*, 56 (2008), 3754–3760
- ²² J. Svoboda, E. Gamsjager, F. D. Fischer, Y. Liu, E. Kozeschnik, *Acta Materialia*, 59 (2011), 4775–4786
- ²³ L. V. Fausett, *Applied Numerical Analysis Using Matlab*, Prentice Hall, New Jersey 1999
- ²⁴ J. W. Thomas, *Numerical partial differential equations: Texts in Applied Mathematics*, vol. 33, Springer, New York 1999
- ²⁵ P. B. Friehling, F. W. Poulsen, M. A. J. Somers, *Z. Metallkd*, 92 (2001), 589–593
- ²⁶ S. Jegou, L. Barralier, R. Kubler, *Acta Materialia*, 58 (2010), 2666–2676
- ²⁷ H. C. F. Rozendaal, E. J. Mittemeijer, P. F. Colijn, P. J. Van Der Schaff, *Metallurgical and Materials Transactions A*, 14A (1983), 395–399